electronics

MDPI

Article

Multi-Stage Hybrid Planning Method for Charging Stations Based on Graph Auto-Encoder

Andrew Y. Wu [1], Juai Wu [2,*] and Yui-yip Lau [1]

[1] School of Professional Education and Executive Development, The Hong Kong Polytechnic University, Hong Kong, China; andrew.wu@cpce-polyu.edu.hk (A.Y.W.); yuiyip.lau@cpce-polyu.edu.hk (Y.-y.L.)
[2] College of Automation & College of Artificial Intelligence, Nanjing University of Posts and Telecommunications, Nanjing 210023, China
* Correspondence: wujuai@njupt.edu.cn

Abstract: To improve the operational efficiency of electric vehicle (EV) charging infrastructure, this paper proposes a multi-stage hybrid planning method for charging stations (CSs) based on graph auto-encoder (GAE). First, the network topology and dynamic interaction process of the coupled "Vehicle-Station-Network" system are characterized as a graph-structured model. Second, in the first stage, a GAE-based deep neural network is used to learn the graph-structured model and identify and classify different charging station (CS) types for the network nodes of the coupled system topology. The candidate CS set is screened out, including fast-charging stations (FCSs), fast-medium-charging stations, medium-charging stations, and slow-charging stations. Then, in the second stage, the candidate CS set is re-optimized using a traditional swarm intelligence algorithm, considering the interests of multiple parties in CS construction. The optimal CS locations and charging pile configurations are determined. Finally, case studies are conducted within a practical traffic zone in Hong Kong, China. The existing CS planning methods rely on simulation topology, which makes it difficult to realize efficient collaboration of charging networks. However, the proposed scheme is based on the realistic geographical space and large-scale traffic topology. The scheme determines the station and pile configuration through multi-stage planning. With the help of an artificial intelligence (AI) algorithm, the user behavior characteristics are captured adaptively, and the distribution rule of established CSs is extracted to provide support for the planning of new CSs. The research results will help the power and transportation departments to reasonably plan charging facilities and promote the coordinated development of EV industry, energy, and transportation systems.

Keywords: electric vehicle charging infrastructure; charging station; multi-stage hybrid planning method; coupled system; graph auto-encoder; graph-structured model

Academic Editor: Felipe Jiménez

Received: 21 November 2024
Revised: 17 December 2024
Accepted: 25 December 2024
Published: 30 December 2024

Citation: Wu, A.Y.; Wu, J.; Lau, Y.-y. Multi-Stage Hybrid Planning Method for Charging Stations Based on Graph Auto-Encoder. *Electronics* **2025**, *14*, 114. https://doi.org/10.3390/electronics14010114

1. Introduction

1.1. Motivation

Exploring the electrification of transportation is a key strategy for achieving "peak carbon" and "carbon neutrality". Consequently, many government agencies worldwide actively promote the adoption of electric vehicles (EVs) and the development of charging infrastructure [1]. As of July 2024, the number of EVs in Hong Kong, China is 98,000, a year-on-year increase of 13.13%, and the increase in charging infrastructure is 7415, a year-on-year increase of 7.23%.

However, the EVs industry currently exposes many prominent problems [2]. On the one hand, the imbalance of the vehicle-to-pile ratio (vehicle-to-pile ratio is the ratio of the

number of EVs in a specific area to the number of charging piles. It is a key indicator to evaluate the suitability of EV charging infrastructure construction and vehicle ownership.) has led vehicle owners to suffer from "charging anxiety" during trips. EV owners often face the dilemma that their vehicles are running out of power while it is difficult to find available charging piles, which disrupts their travel plans and aggravates their concerns about battery life. On the other hand, the utilization of charging stations (CSs) shows a polarized trend. Some CSs are overcrowded, and vehicle owners have to wait in line for an unexpectedly long time, greatly reducing the charging efficiency. In sharp contrast, some other CSs are rarely visited, and a large number of idle zombie piles exist, resulting in a serious waste of charging resources. Given that urban fast-charging stations (FCSs) play a crucial role as energy supply nodes in the urban transportation electrification coupling network, to effectively address the above problems, it is imperative to optimize the regional layout and capacity configuration of FCSs. Specifically, it is necessary to fully consider factors such as the number of EVs in different regions, peak travel periods, and traffic flow, and conduct precise planning, to effectively improve the utilization rate and service level of charging facilities, thereby promoting the efficient integration of charging resources and facilitating the all-round upgrading of the EVs ecosystem.

1.2. Literature Review

Until now, many scholars have conducted extensive research on planning schemes for CSs. They strive to improve the overall CS service efficiency by optimizing the CS locations and charging pile configurations. Based on an in-depth analysis of the intrinsic connection between charging demand and CS planning, references [3–5] propose differentiated planning strategies for CSs. The authors of [3] developed an optimization framework based on a genetic algorithm to weigh the relationship between the equilibrium distribution of charging demand and the deployment cost of CSs. The literature [4] develops a prediction model for EV charging behavior, focusing on the dynamic characteristics of EV charging demand. It analyzes urban charging thermal regions and offers decision-making support for the location and capacity of CSs. In the literature [5], a cross-field integrated planning method is adopted to comprehensively consider the effective matching between charging demand and power supply. A flexible planning scheme adapted to different penetration rates of EVs is formulated. The above-mentioned approaches aim to improve the efficiency of charging services by optimizing the location of CSs and the configuration of charging piles. However, the research mainly focuses on theoretical simulations of small-scale topologies, resulting in certain discrepancies between the results and actual planning schemes.

Other studies [6–8] synergistically consider the joint planning of CSs and power networks, mainly by optimizing the layout of CSs and the allocation of power resources to improve the operational efficiency of the coupled network. For example, based on the collaborative planning of CS construction and power distribution systems, two studies [6,7] propose a joint planning model of FCSs and power distribution systems to prevent charging network congestion caused by CS construction. Further, the literature [8] proposes a planning model for CSs and power grid topology reconstruction to optimize the construction scheme of CSs and power grid lines, ensure the safe operation of power grids, and reduce equipment investment costs. The above-mentioned methods improve the efficiency of the coupling network by optimizing the layout of CSs and resource allocation of charging facilities. However, the research only focuses on the optimization of the coupling network. Regarding the determination of the geographical location and number of CSs, these methods fail to fully consider the comprehensive impact of the 'vehicle-station-network' correlation factors.

Further, these scholars [9–12] develop a cooperative planning model for CSs. This model takes into account the dynamic equilibrium of traffic flow and optimizes the layout of CSs. It is centered around the cooperative and optimal operation of traffic-electrical coupling networks. The authors of [9] present a user equilibrium model to predict EV charging flow and propose a planning method for integrating urban transportation networks (TNs) with charging networks. This approach aims to determine the location and size of fixed CSs in electrified transportation systems to minimize overall travel time and investment costs. The authors of [10] establish a long-term planning model for optimal CSs to achieve a dynamic balance between traffic flow and charging demand. The authors of [11] consider the traffic flow balance regulation method of road capacity expansion and establish an unconstrained traffic allocation model and CSs location model to determine the best candidate location of CSs. The authors of [12] discuss the impact of dynamic traffic balancing on the operation of CSs in-depth and build a two-stage stochastic programming dynamic traffic balancing model. By predicting and optimizing the charging behavior of users, the waiting time of users is shortened, and the response speed and efficiency of CS services are improved. The above-mentioned methods consider the dynamic balance of traffic flow. These models take the cooperation of the traffic-power coupling network as the core to optimize the layout of CSs. However, the models' ability to process multi-source data is limited, failing to accurately and efficiently determine the suitable geographic location and number of CSs.

Additionally, studies [13–15] focus on establishing a CS locations optimization model to reduce user charging costs and improve the operating efficiency of CSs. The authors of [13] establish the M/M/s/N queuing model to reduce user waiting time and traffic congestion probability. It also adopts a capacity planning model of CS integrating fuzzy service quality and multiple charging options to effectively reduce the service cost of CSs. The authors of [14] introduce a centralized CS data management system to coordinate the charging behavior of various vehicles and reduce the waiting time of EV owners at CSs by rationally planning the geographical location of urban FCSs. The authors of [15] propose a CS siting model for electric buses to simulate the nonlinear charging characteristics of electric bus batteries and to achieve the minimization of CS reduction costs while ensuring charging service levels. The above-mentioned research effectively reduces the service cost of charging stations by integrating fuzzy service quality and planning the geographical location of urban CSs. However, the above-mentioned research lacks the ability to capture the complex and changeable behavioral characteristics of users and accurately extract the distribution rules of built CSs under different geographical environments, traffic modes, and user needs.

Although the above-mentioned methods play an important role in the CS locations and charging facilities configurations, the traditional modeling methods mostly use simulation topology for static planning and fail to consider the complex influencing factors of CS planning decision-making. The limited scale of the planning scheme makes it difficult to match the rapid expansion of the EV market and the dynamic evolution of charging demand.

The application of AI techniques, particularly deep learning and reinforcement learning methods, is increasingly becoming a focal point in CS planning research. AI techniques dynamically capture various factors influencing CS layout and operational strategies. It efficiently addresses complex decision-making problems involving multimodal data and multidimensional variable inputs, showcasing exceptional computational capabilities.

Aiming at the elastic load of users charging and the optimal planning of CSs, several studies [16–18] apply deep learning to predict charging flow in networks and subsequently determine appropriate CS sizes. In this study [16], the encoder-decoder depth architecture

based on multi-relationship graph convolutional networks is used to evaluate the spatiotemporal load of EVs and to solve the optimal planning model of charging infrastructure. Similarly, the authors of [17] construct a day-ahead energy demand forecasting model, integrating a long short-term memory model with Stackelberg game theory to devise an optimal siting and pricing strategy for CSs. The authors of [18] explore the problem of EV charging infrastructure planning based on a trained recurrent neural network model under an unknown spatial correlation within the charging network.

Further, to capture users' random charging and drive behavior patterns and analyze how the behavior patterns affect the flow orientation and location optimization of CSs, various scholars [19,20] have developed an intelligent decision-making framework for FCSs by using deep reinforcement learning (DRL) algorithms. The authors of [19] analyze the sensitivity of traffic flow and charging demand to the FCS planning scheme and, based on the multi-agent DRL algorithm, jointly developed charging guidance for EVs users and the CS locations and charging pile configurations refinement scheme of CSs. The authors of [20] use DRL to learn charging and driving decision-making of EVs under differentiated traffic network topology and FCS planning scheme and build a data-driven proxy planning framework to optimize the CS locations and charging pile configurations.

Other scholars [21–23] focus on applying DRL methods to address the multidimensional decision-making problems in CS planning. In [21], a recurrent neural network with an integrated attention mechanism is used to learn model parameters and determine optimal strategies through unsupervised learning to realize the optimal deployment of FCSs. A study [22] proposes an asymptotic planning scheme to dynamically expand EV charging resources. This variable CS planning scheme is enhanced by incorporating an attention mechanism and an expansion factor. In [23], a dominant actor-critic (A2C) DRL method is applied to areas with high traffic density and high new energy potential. A randomized start search method is used to identify optimal sites in complex urban environments and evaluate the capacity of potential FCSs.

1.3. Research Gap and Contributions

Regarding the advanced CS planning methods in this field, there are still two significant limitations:

First, most AI-based CS planning studies do not fully explore the graph-structured interaction characteristics of the coupled "Vehicle-Station-Network" system. They mostly rely on the temporal information of the coupled system as an influencing factor for planning decision-making.

Second, existing CS planning models do not comprehensively assess the variability of urban functional areas and the charging demand of different users. These models lack the CS locations and charging pile configurations refinement scheme for developing a complete set of fast-slow charging combinations, which cannot provide decision-making support for the expansion construction of the real-world EV charging network.

To this end, this paper proposes a novel AI scheme based on a graph auto-encoder to solve the multi-stage hybrid planning problem of urban CSs. In the first stage, a graph auto-encoder is used to identify the types of CSs of urban topology nodes. Based on the realistic geographical space and large-scale traffic topology, the method comprehensively considers the multi-information interaction process, realizing the adaptive capture of user behavior characteristics. The proposed method accurately captures the dynamic changes of urban traffic networks and the complex relationship between nodes and effectively obtains the set of candidate CSs. In the second stage, the traditional optimization method is used to model the multi-agent cost of candidate CSs. This method comprehensively considers

the costs and benefits of different stakeholders and establishes the optimal station location and charging pile configuration. The main contributions of this paper are threefold:

1. The combination architecture of DRL and traditional intelligent optimization is proposed, and a multi-stage optimization model is constructed to solve the CS planning and decision-making problem. The GAE is used to process the identification and classification of network topology, and the feasible candidate CS is efficiently screened out from a large number of topology nodes. The traditional intelligent optimization method comprehensively considers the interests of multiple parties, re-optimizes the candidate CS set, and improves the decision-making effect of determining the optimal CS locations and charging pile configurations.
2. The coupled "vehicle-station-network" system is constructed as a graph-structured model. Multi-subject interaction, network topology, and temporal information of the coupled system are unified and characterized as embedded features in the graph topology. It better helps the neural network capture topological and spatial correlation, and effectively improve the learning efficiency of multi-dimensional feature data.
3. Under the urban traffic topology architecture, we use real-world data to test the planning of CSs in the selected areas, more realistically exploring the characteristics of the functional area and reflecting the user charging willingness. The testing results show that the proposed method not only improves the operation efficiency of the EV charging network but also reduces the charging cost of users.

1.4. Paper Organization

The remainder of this paper is organized as follows. Section 2 describes the modeling process for multi-stage hybrid planning for CSs. Then our solution is presented in Section 3. Case studies are reported to assess our proposed methodology in Section 4. Finally, Section 5 summarizes the whole paper.

2. Overall Architecture

Figure 1 is the overall architecture of the multi-stage hybrid planning method for CSs. As shown in Figure 1, a multi-stage hybrid optimal siting and sizing method for CSs is constructed, considering the interaction of EVs, CSs, and TNs. The model explicitly includes a graph-structured representation module, a GAE-based candidate CS node identification module (first stage), and an optimal hybrid CS planning evaluation module (second stage).

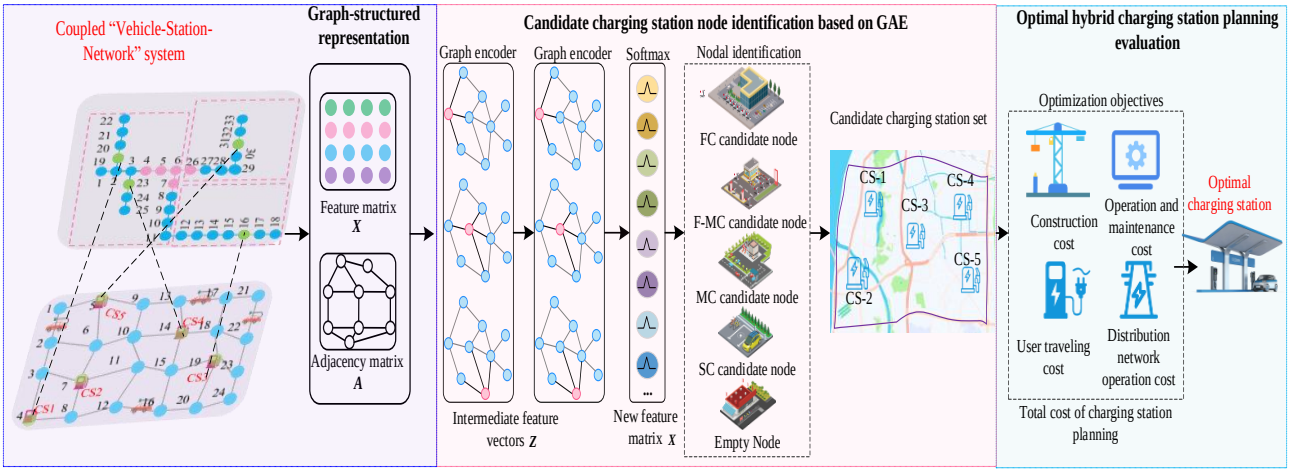

Figure 1. Overall architecture of the proposed multi-stage hybrid planning method for CSs.

The graph-structured representation module's inputs encompass the topology and environmental information of the coupled "Vehicle-Station-Network" system. The adjacency matrix and feature matrix are derived from graph-structured modeling, characterizing connectivity and information interaction among multiple subjects of the coupled system, serving as inputs for the GAE module.

Based on the GAE module, the embedded feature knowledge of graph topology is implicitly learned, and the topological node type recognition results are output, including FCS nodes, fast-medium-charging station (FMCS) nodes, medium-charging station (MCS) nodes, slow-charging station (SCS) nodes, and empty nodes. The node recognition results are constructed as a candidate CS set.

Finally, the evaluation module comprehensively screens the candidate CS set. The traditional algorithm based on particle swarm optimization (PSO) is used to construct the optimization objectives and constraints and determine the planning location of the optimal CS within the region and the configuration of different types of charging piles.

3. Problem Modelling

3.1. Graph-Structured Representation of the Couped "Vehicle–Station–Grid" System

To realize feature modeling and environment information extraction for the coupled system, we introduce the graph-structured representation modeling method for graph topology knowledge learning. For the coupled system $\boldsymbol{G}^{\mathrm{VSN}}$, the graph-structured form is denoted as $\boldsymbol{G}^{\mathrm{VSN}} = (\boldsymbol{A}, \boldsymbol{X})$. $\boldsymbol{A} \in \mathbb{R}^{M \times M}$ is the adjacency matrix of the coupled system $\boldsymbol{G}^{\mathrm{VSN}}$, characterizing the connection relationship among EVs, CSs, and TNs. M denotes the number of nodes of the coupled system. If there is a connection between nodes v_i and v_j of the coupled system $\boldsymbol{G}^{\mathrm{VSN}}$, the matrix element can be denoted $\boldsymbol{A}_{ij} = 1$. Otherwise $\boldsymbol{A}_{ij} = 0$. The topological model of the coupled system $\boldsymbol{G}^{\mathrm{VSN}} = (\boldsymbol{A}, \boldsymbol{X})$ is shown below [24].

$$\boldsymbol{A} = \begin{bmatrix} \mathrm{V} & \mathrm{V\text{-}S} & \mathrm{V\text{-}N} \\ \mathrm{S\text{-}V} & \mathrm{S} & \mathrm{S\text{-}N} \\ \mathrm{N\text{-}V} & \mathrm{N\text{-}S} & \mathrm{N} \end{bmatrix} \tag{1}$$

where both V and S are unit matrices, representing the dimensions of EVs and CSs, respectively. N represents the topological connectivity matrix of traffic roads. Both V-N and N-V denote the physical connectivity between EVs and TNs. They are used to track the trajectories of EVs in the road networks. Both S-N and N-S denote the physical connectivity between CSs and TNs, which are used to locate the real-world geographical location of CSs. Both V-S and S-V denote the electrical connection relationship between EVs and CSs, which are used to describe the EV receiving charging service at the CS.

Further, $\boldsymbol{X} \in \mathbb{R}^{N \times C}$ denotes a feature matrix for storing the energy and information interaction features of the environment. C represents the number of features of each node. To avoid mis-identification of the node features, the feature vector is expanded according to the sum of the dimensions of the features for each type of subjects, and the basic form can be expressed as $\boldsymbol{X} = [\boldsymbol{V}, \boldsymbol{S}, \boldsymbol{N}]$.

$$\begin{cases} \boldsymbol{V}_{t,i} = \left[t_i^{init}, p_i^{init}, s_i^{bat}, \varphi_i^{will} \right] \\ \boldsymbol{S}_{t,j} = \left[s_j, p_j^{init}, P_j^{ch}, \omega_{t,j}, H_j^{wait} \right] \\ \boldsymbol{N}_{t,m} = \left[POI_m, l_{mn}, w_{mn}, v_{mn}^{e} \right] \end{cases} \tag{2}$$

where $t^{init}, v^{\mathrm{init}}, s^{bat}, \varphi^{will}$ denote the instant time, instant location, EV battery SOC, and owner's charging willingness, respectively. $s^{\mathrm{CS}}, \psi^{\mathrm{CS}}, I^{\mathrm{CS}}, P^{\mathrm{ch}}, \omega^{\mathrm{CS}}, T^{\mathrm{CS}}, A^{\mathrm{sta}}$ denote the number of charging piles of CSs, location of CSs, type of CSs charging power of charging

piles, charging tariff, average waiting time and floor space, respectively. $\varphi^{\mathrm{TN}}, l^{\mathrm{TN}}, w^{\mathrm{TN}}, v^{\mathrm{TN}}$ denote the point of interest for the node, the length of the traffic segment, the class of the traffic segment and the traffic speed, respectively.

3.2. GAE-Based Identification for Candidate CS Nodes

The graph-structured model $\boldsymbol{G}^{\mathrm{VSN}} = (\boldsymbol{A}, \boldsymbol{X})$ is obtained as the input to the GAE module. The graph encoder of the GAE module is utilized to differentiate the interconnections between topological nodes. The intermediate feature vector $\widetilde{\boldsymbol{Z}}$ reflecting the embedded feature information of important nodes is obtained. Then, the graph decoder of the GAE module is used to reconstruct and classify the intermediate feature vector $\widetilde{\boldsymbol{Z}}$, obtaining the new feature matrix $\widetilde{\boldsymbol{X}}^{1\times M}$. Namely, all the nodes in the coupled system are labeled for identification and classification. The new feature matrix $\widetilde{\boldsymbol{X}}^{1\times M}$ is used as the candidate CS set. The specific implementation is as follows.

The graph encoder uses a graph convolutional neural network to perform self-circular transformation and normalization on the adjacency matrix $\boldsymbol{A}$, obtaining a normalized adjacency matrix $\boldsymbol{A}''$.

$$\boldsymbol{A}' = \boldsymbol{A} + \boldsymbol{I} \tag{3}$$

$$\boldsymbol{A}'' = \boldsymbol{D}^{-\frac{1}{2}}\boldsymbol{A}'\boldsymbol{D}^{-\frac{1}{2}} \tag{4}$$

where $\boldsymbol{A}'$ denotes the self-cyclic adjacency matrix. $\boldsymbol{I} \in \mathbb{R}^{M\times M}$ denotes the unit matrix. $\boldsymbol{D}$ denotes the diagonal node degree matrix of the self-cyclic adjacency matrix $\boldsymbol{A}'$.

The output $\widetilde{\boldsymbol{Z}} \in \mathbb{R}^{N\times F}$ can be obtained by performing a graph convolution transform on the obtained normalized adjacency matrix $\boldsymbol{A}''$ and the feature matrix $\boldsymbol{X}$. F denotes the number of features in each node of the obtained intermediate feature vector $\widetilde{\boldsymbol{Z}}$. Each graph convolution layer is represented by a nonlinear activation function $\sigma(\cdot)$ as follows [25].

$$\boldsymbol{H}_{i+1} = \sigma(\boldsymbol{H}_i, \boldsymbol{A}'') \tag{5}$$

where $i = 0, 1, \ldots, L$, L is the number of graph convolution layers (GCLs). When $i = 0$, $\boldsymbol{H}_0$ is identical to $\boldsymbol{X}$. When $i = L$, $\boldsymbol{H}_l$ is identical to $\widetilde{\boldsymbol{Z}}$. $f(\cdot)$ denotes the graph convolution operation. $\boldsymbol{W}_i \in \mathbb{R}^{C\times F}$ is the weight matrix of the ith graph convolution layer.

$$f(\boldsymbol{H}_i, \boldsymbol{A}'') = \sigma(\boldsymbol{A}''\boldsymbol{H}_i\boldsymbol{W}_i) \tag{6}$$

The graph decoder is reconstructed using the inner product to get the new feature matrix $\widetilde{\boldsymbol{X}}^{1\times M}$. $\sigma(\cdot)$ is a sigmoid function as shown in Equation (7).

$$\widetilde{\boldsymbol{A}} = \sigma(\widetilde{\boldsymbol{X}}\widetilde{\boldsymbol{X}}^{T}) \tag{7}$$

The loss function $\mathcal{L}$ is computed using cross-entropy.

$$\mathcal{L} = -\frac{1}{N}\sum_{y\in A} y\log\widetilde{y} + (1-y)\log(1-\widetilde{y}) \tag{8}$$

where: y is the element of the feature matrix. $\widetilde{y}$ is the element of the new feature matrix.

3.3. Hybrid Planning Evaluation for Optimal CSs

3.3.1. Objective Function

In this paper, the sum of CS construction cost, operation and maintenance cost, user traveling cost and distribution network operation cost is chosen as the total cost of CS planning C [26], as below.

$$\min C = \sum_{n=1}^{N} \left(C_n^{\text{cons}} + C_n^{\text{oper}} + C_n^{\text{user}} \right) + C^{\text{grid}} \tag{9}$$

where C_n^{con} is the construction cost of the nth CS. C_n^{ope} is the operation and maintenance cost of the nth CS. C_n^{user} is the traveling cost of the nth CS for EV users. C^{grid} is the operation cost of the distribution network. $n = 1, 2, \ldots, N$, N is the number of CSs.

a. CS construction costs

The CS construction cost C_n^{con} consists of the basic investment cost C_n^{inv} of the CS and the acquisition cost C_n^{purc} of the charging pile.

$$C_n^{\text{con}} = C_n^{\text{inv}} + C_n^{\text{purc}} \tag{10}$$

The basic investment cost C_n^{inv} of the CS mainly includes the cost of land lease, road gate construction, and charger installation.

$$C_n^{\text{inv}} = \tau_0 (1 + \tau_0)^T \frac{(A_n^{\text{sta}} C_n^{\text{pri}} + C_n^{\text{dev}})}{(1 + \tau_0)^T - 1} \tag{11}$$

where τ_0 is the discount rate. T is the planning period. A_n^{sta} is the CS footprint. C_n^{pri} is the CS location equivalent investment construction unit price. C_n^{dev} is the charging infrastructure construction cost.

The acquisition cost C_n^{purc} of charging piles depends on the type and quantity. Therefore, the acquisition cost of the charging piles in the nth CS is expressed as follows:

$$C_n^{\text{purc}} = C^{\text{high}} N_n^{\text{hc}} + C^{\text{med}} N_n^{\text{mc}} + C^{\text{low}} N_n^{\text{lc}} \tag{12}$$

where C^{high}, C^{med}, and C^{low} are the unit prices of fast, medium, and slow charging piles, respectively. N_n^{hc}, N_n^{mc}, and N_n^{lc} are the numbers of fast, medium, and slow charging piles, respectively.

b. CS operation and maintenance costs

The operation and maintenance costs C_n^{ope} of the CS, including the depreciation of the charger as well as the operation and maintenance of the hardware and software, are taken as a percentage (conversion factor λ) of the initial construction investment, as follows:

$$C_n^{\text{ope}} = \lambda (A_n^{\text{sta}} C_n^{\text{pri}} + C_n^{\text{dev}}) \tag{13}$$

c. User traveling costs

The user cost C_n^{user} includes the en-route charging loss cost C^{tra} and queuing waiting time cost C^{wait}.

$$C_n^{\text{user}} = C^{\text{tra}} + C^{\text{wait}} \tag{14}$$

$$C^{\text{tra}} = 365\beta \sum_{n=1}^{N} \sum_{m=1}^{M} \Delta T \tag{15}$$

$$C^{\text{wait}} = 365\omega \sum_{n=1}^{N} \sum_{t=1}^{24} T_t n_t \tag{16}$$

where β is the unit time cost of urban traveling. M and ΔT are the number of charging demands within the service range of the nth CS and the EV traveling time from its current location to the CS, respectively. w is the hourly queuing cost of the user. T_t is the average queuing time of the nth CS at time t. n_t is the number of EV charging demands within the service range of the nth CS at time t.

d. Distribution network operation costs

Since the CS construction requires electric energy, the distribution network party needs to build a new power line between the CS and the grid to obtain electric energy. Moreover, the CS access to the grid will cause an increase in the active network loss, which corresponds to the annual cost of the distribution network:

$$C^{\text{grid}} = 8760\varpi\left(P^{\text{init}} - P^{\text{late}}\right) + \sum_{n=1}^{N} l^{\text{grid}} c^{\text{grid}} \frac{r_0(1+r_0)^y}{(1+r_0)^y - 1} \tag{17}$$

where C^{grid} is the annual network loss cost added to the distribution network after accessing the CS load. l^{grid} is the length of the new line of the nth CS accessing the corresponding distribution network node. c^{grid} is the line unit price. c^{grid} is the initial active network loss of the distribution network. P^{init} is the active network loss after accessing the CS load of the distribution network. ϖ is the unit price of electricity.

3.3.2. Constraints

a. Number of CS constraint

The number N of CSs in the area to be planned determines the economic benefits for both the CSs and the users and is related to the upper and lower limits of the charging demand and CS capacity in the area, which is constrained by the following equation.

$$N_{\min} \leq N \leq N_{\max} \tag{18}$$

where $N_{\min}$ is the minimum number of CSs. $N_{\max}$ is the maximum number of CSs.

b. Charging power constraints

The charging power P_n of the nth CS is determined by the number of EV charging demands n_t and the rated power of the charging pile p^{pile} at time t.

$$P_n = p^{\text{pile}} \sum_{n=1}^{N} \sum_{t=1}^{24} n_t \tag{19}$$

c. Distribution network node voltage constraints

The charging distribution network node voltages satisfy the following constraints:

$$U_g^{\min} \le U_g \le U_g^{\max} \tag{20}$$

where U_g is the voltage magnitude at node g in the distribution network. $U_g^{\min}$ and $U_g^{\max}$ are the maximum and minimum voltage magnitudes at node g in the distribution network, respectively.

d. Distribution network node capacity constraints for accessing CS loads

The distribution network node capacity constraints for accessing CS loads must satisfy the following constraints:

$$P_{n,g} + P_g \le P_{g,\,\max} \tag{21}$$

where $P_{n,g}$ is the charging load of the nth CS connected to the distribution network node g. P_g is the load of the distribution network node g. $P_{g,\,\max}$ is the maximum load allowed to be connected to the distribution network node g.

Power flow constraints of the distribution network

The power flow in the distribution network satisfies the following constraints:

$$\begin{cases} P_g = U_g \sum U_h \left(G_{gh} \cos\theta_{gh} + B_{gh} \sin\theta_{gh} \right) \\ Q_g = U_g \sum U_h \left(G_{gh} \sin\theta_{gh} - B_{gh} \cos\theta_{gh} \right) \end{cases} \tag{22}$$

where P_g and Q_g represent the active and reactive power at node g, respectively. U_h is the voltage at node h. G_{gh} and B_{gh} denote the conductance in branch gh, respectively. θ_{gh} indicates the difference in phase angle between nodes g and h.

4. GAE and PSO-Based Solution Method

The pseudo-code of the multi-stage hybrid planning method for CSs based on GAE-PSO is shown in Algorithm 1.

Firstly, based on the GAT module, graph-structured modeling and node identification are performed on the topological information and feature information until all node labels of the coupled system are classified. The candidate CS set $\widetilde{\boldsymbol{X}}^{1\times M}$ is obtained.

Then, based on the PSO module, the optimal CS planning scheme is completed. The position μ and velocity ν of the particle swarm are updated. The objective function of each particle swarm is calculated. The historical optimal value of each particle swarm and the optimal value of the entire particle swarm are updated. The above steps are repeated until the maximum number of iterations is reached.

Finally, the total cost of the CS planning and the corresponding decision-making plan are output.

Algorithm 1. GAE-PSO-based Multi-Stage Hybrid Planning Method for CSs

1. **Initialization:** number of graph convolution layers $\boldsymbol{L}$, adjacency judgment function $\theta(v_i, v_j)$, network parameter ω, learning rate, position μ, velocity v
2. **For** node $v_i \in \boldsymbol{A}$ do
3. **For** node $v_j \in \boldsymbol{A}$ do
4. **If** $\theta(v_i, v_j)$
5. Compute the elements of the adjacency matrix $A_{ij} = 1$
6. **Else if**
7. Compute the elements of the adjacency matrix $A_{ij} = 0$
8. **End if**
9. **End for**
10. **End for**
11. Compute the self-circular transformation adjacency matrix $\boldsymbol{A}' = \boldsymbol{A} + \boldsymbol{I}$
12. Compute the normalized adjacency matrix $\boldsymbol{A}'' = \boldsymbol{D}^{-\frac{1}{2}}\boldsymbol{A}'\boldsymbol{D}^{-\frac{1}{2}}$
13. **For** i = 0 to L do
14. $f(\boldsymbol{H}_i, \boldsymbol{A}'') = \sigma(\boldsymbol{A}''\boldsymbol{H}_i\boldsymbol{W}_i)$
15. $\boldsymbol{X} = \sigma(\boldsymbol{Z}\boldsymbol{Z}^T)$
16. **End for**
17. Output candidate CS set $\boldsymbol{X}^{1\times M}$
18. **For** k steps do
19. Updating the location μ and velocity v
20. Calculate the objective function C for each particle swarm min
21. Update the historical optimal values of each group of particle swarms and the optimal values of all particle swarms
22. **End for**
23. Output total costs and corresponding solutions of CS planning

5. Case Study

5.1. Experimental Setup

In this study, the performance of the proposed approach is illustrated using a real-size urban zone in Kowloon City District, Hong Kong, China. The selected area covers approximately 10 km^2, which contains includes 523 transportation nodes and 50 CSs. A modified IEEE-123 node distribution system, with a reference voltage of 4.16 kV and a total network load of 1.40 + j0.77 MW, is used to align with the transportation network size. Real-time operation data for urban roads is obtained from 'Open Street Map', while configuration and operational data for EVs and CSs are sourced from 'Charge Bar'. Data collected from 1 November to 30 November 2023 are used for the experiments. The first 25 days serve as training samples, and the last 5 days are testing samples. The main parameters of the approach are presented in Appendix A Table A1. Experiments are conducted on a server with an R93950X CPU, RTX 2080TI GPU, 32 GB RAM, and PyCharm-2024 simulation software.

5.2. Training Process

This study separately trains the model under different GCLs to examine the influence on feature recognition. The training convergence curve is shown in Figure 2, where

the learning rate is 0.001 and the batch size is 32. Adam is chosen as the optimizer. From Figure 2, the loss functions for different GCLs converge after approximately 70 to 90 episodes. When the number of GCLs is 2, the average loss after stabilization is 0.0065. As the number of layers increases, the loss function stabilizes around 0.006. However, more GCLs require exponential growth in the amount of aggregated neighbor node information, which not only makes node features smoother and loses diversity but also increases the computational complexity of the model. In summary, balancing model feature aggregation performance and computational complexity, this paper selects 2-GCL for the experiment.

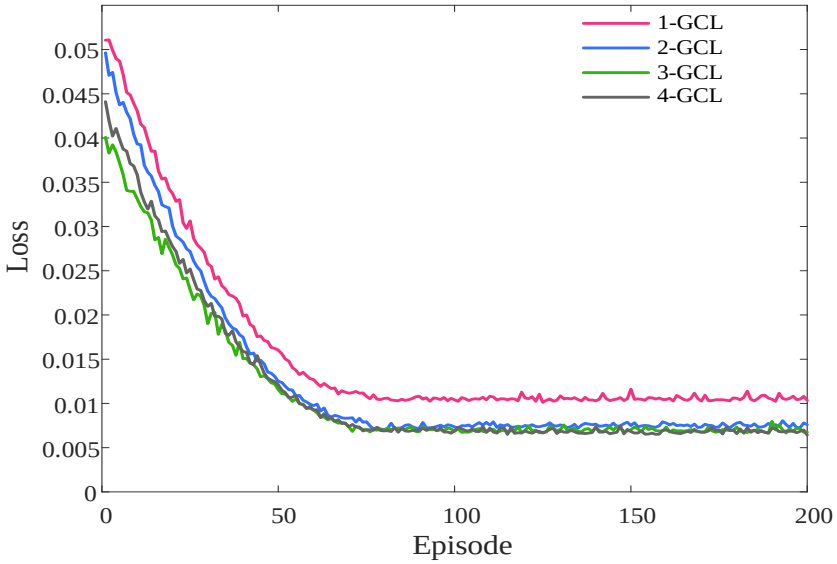

Figure 2. Loss function for training with different GCLs.

Further, to verify the accuracy of the GAE model, 2-GAL is selected. The validation set is used for simulation and the training classification accuracy curve is shown in Figure 3.

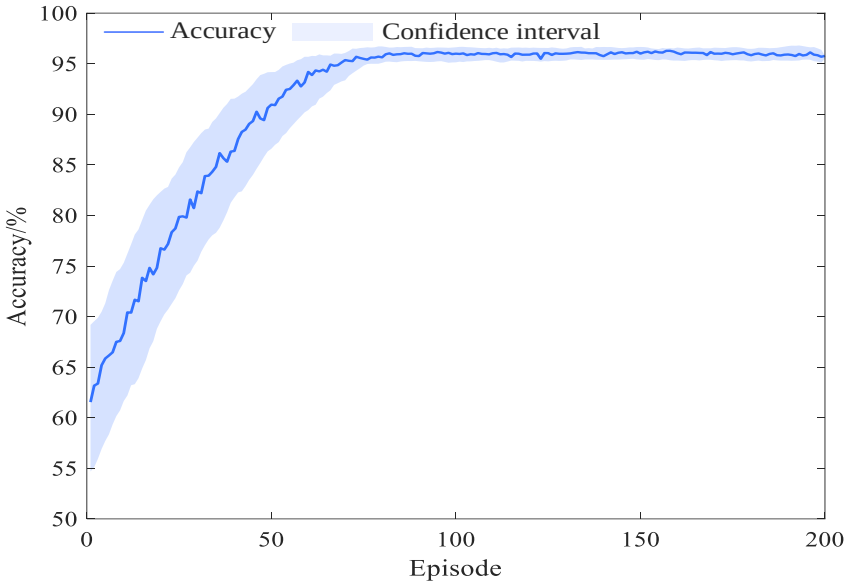

Figure 3. Classification accuracy of the proposed GAE method for candidate CS nodes.

As shown in Figure 3, the training accuracy curve goes through two phases of rapid increase and stable convergence. During the early training phase, the classification accuracy increases rapidly with the number of episodes. In this phase, the topology as well as the information interactions of CSs are quickly captured based on the GAE module to

better categorize the topology nodes. After approximately 100 episodes, the classification accuracy curve stabilizes, achieving an average accuracy of 94.82%. This demonstrates the ability of the proposed method to accurately classify topological nodes in complex network environments.

5.3. Practical Application Results

The identification result of the candidate CS nodes within the selected area is shown in Figure 4. As depicted, the majority of identified candidate FMC nodes are concentrated in commercial areas, accounting for approximately 40.31%. These areas experience a large demand for fast charging due to significant EV traveling flow. Candidate FMC and MC nodes are primarily located in commercial and industrial areas, such as Stonecutters Island and Whampoa. Candidate SC nodes are relatively few, mostly distributed in residential areas, accounting for only about 12.35%. EV users in these areas travel mainly for commuting and have a greater demand for slow-charging services.

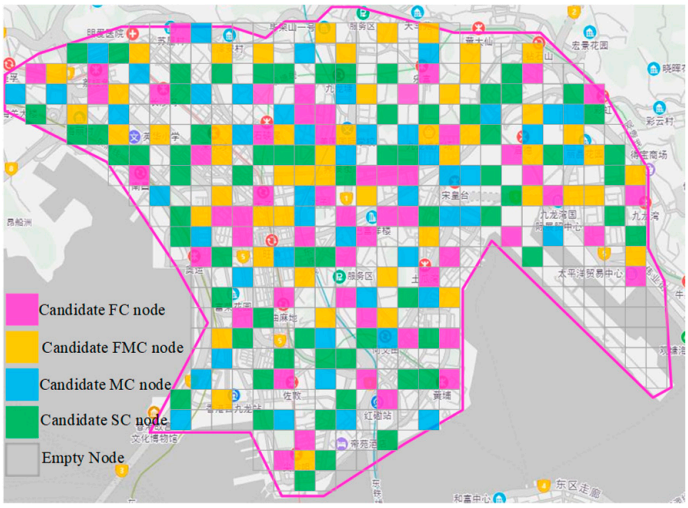

Figure 4. Identification result of the candidate CS nodes.

Next, to determine the relationship between the total cost of CS planning and the number of CS construction, Figure 5 shows the PSO-based iterative process. In addition, the individual-specific costs corresponding to the quantity of CSs are shown in Figure 6.

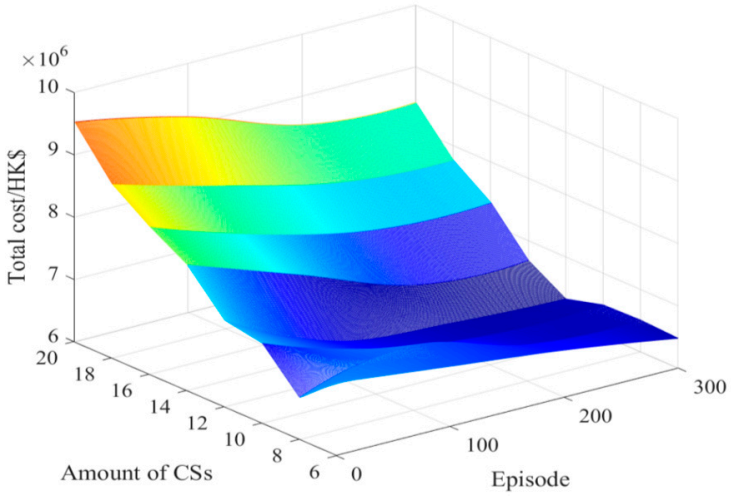

Figure 5. PSO-based iterative process of CS planning.

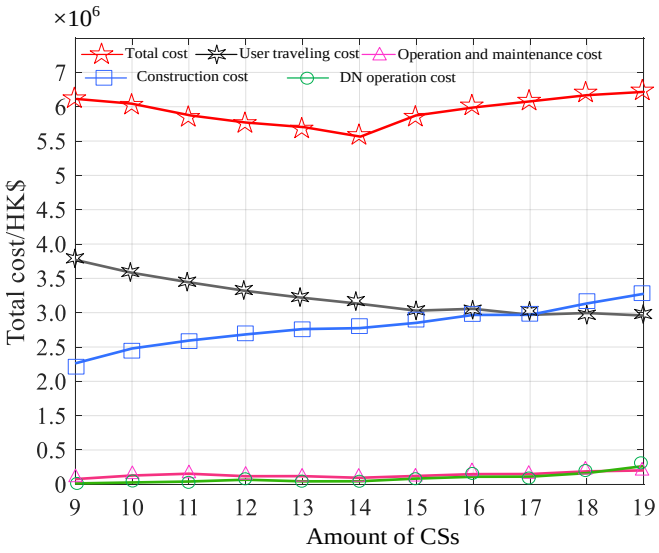

Figure 6. Relationship between the total cost and quantity of CS planning.

Combining Figures 5 and 6, the total planning cost shows a trend of decreasing and then increasing as the number of CSs constructed increases. However, this increase is not strictly linear. Notably, construction costs and user travel costs significantly affect the total planning cost. Specifically, when the number of CSs is set to 14, the total cost reaches its minimum at HKD 5.36 million. Concurrently, user travel costs decrease from HKD 3.85 million to HKD 3.12 million. The increase in the number of CSs has improved the convenience of charging, reduced the charging time and distance for users, and thus reduced traveling costs. Additionally, the operation and maintenance costs and distribution network operating costs have increased, however, the magnitude of changes is relatively small. It shows that proper cost control measures can effectively maintain costs at a low level during the operation of CSs. Overall, during the CS network planning process, our method achieves the optimal balance between cost and benefit by reasonably regulating the number of fast CSs, ensuring user experience while effectively controlling the total cost.

Figure 7 and Table 1 present the results of the optimal hybrid planning and charging pile configurations of 14 CSs. The figure shows that the planning results include five FCSs, four FMCSs, three MCSs, and two SCSs.

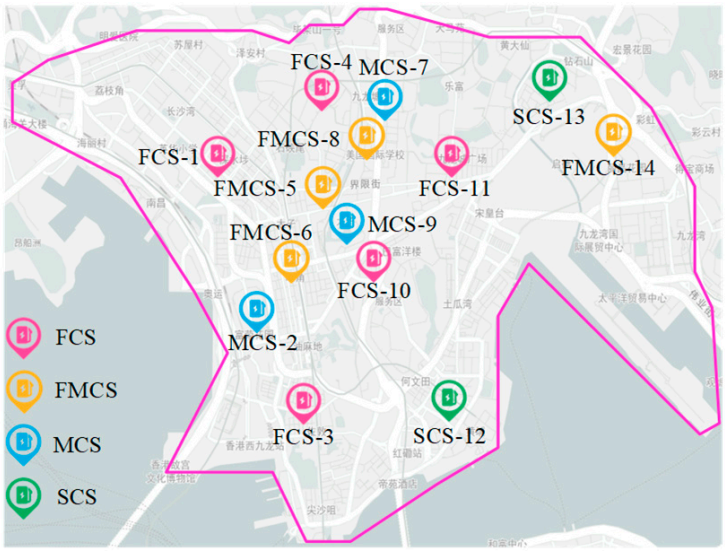

Figure 7. Distribution results of the optimal hybrid planning for CSs.

Table 1. Planning results of the types of CSs and the configuration of charging piles.

Serial Number of CSs	Type of CSs	Number of Charging Piles	Serial Number of CSs	Type of CSs	Number of Charging Piles
1	FCS	15	8	F-MCS	(14, 19)
2	MCS	14	9	MCS	9
3	FCS	12	10	FCS	21
4	FCS	13	11	FCS	16
5	FMCS	(17, 13)	12	SCS	16
6	FMCS	(11, 18)	13	SCS	13
7	MCS	10	14	FMCS	(13, 12)

5.4. Analysis of Pre-Post-Planning for CSs

Additionally, to analyze the planning effect of the charging stations, charging experiments are simulated for 2000 EVs introduced within the selected area. The comparison of the spatial thermal distribution of pre-post planning charging demand is given in Figure 8. The figure shows that the spatial distribution of charging demand before planning is concentrated in the central area, with a peak demand of 3.92 MW. In contrast, the proposed scheme optimizes the locations of CSs, ensuring effective coverage and efficient use of resources. After planning, peak charging demand is reduced by 37.51% compared to the pre-planning period, significantly improving user charging experience and effectively alleviating peak load pressure on the urban power grid.

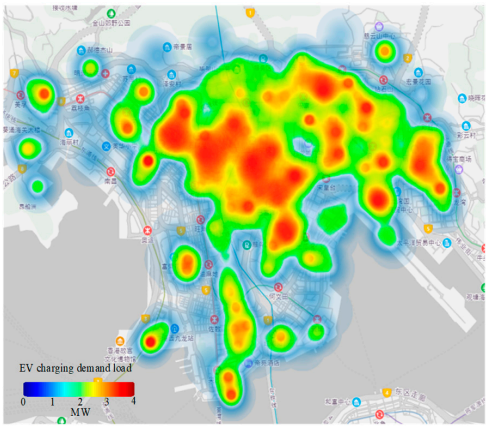

(**a**)

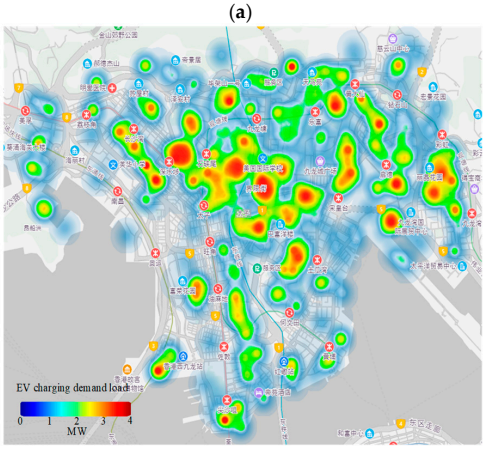

(**b**)

Figure 8. Heat map of spatial distribution of pre-post-planning charging demand. (**a**) Spatial distribution of pre-planning charging demand. (**b**) Spatial distribution of post-planning charging demand.

Further, Figure 9 illustrates the curves of average traveling and charging costs of pre-post-planning, while Table 2 compares various indicators of pre-post-planning. From Figure 9 and Table 2, the average time cost for users is unevenly distributed due to morning and evening traveling peaks, with an average cost of HKD 50.44 before planning. By optimizing the distribution of CS nodes, the proposed method significantly reduces the average time cost for users by 15.27%. Charging costs are primarily influenced by tariffs, with the most significant impact occurring during the evening peak from 19:00 to 20:00. The average charging costs of pre-post-planning are HKD 44.01 and HK$ 34.61, respectively. Furthermore, Table 2 indicates that the waiting time for charging has decreased from 7.88 min to 3.25 min after planning. This reduction not only alleviates charging congestion and enhances user experience but also improves the efficiency of charging facilities, mitigating the issue of "zombie piles" due to prolonged equipment inactivity at some stations. In summary, the implementation of the proposed optimal scheme for CSs not only effectively reduces users' traveling and charging costs but also improves the utilization rate of urban charging piles.

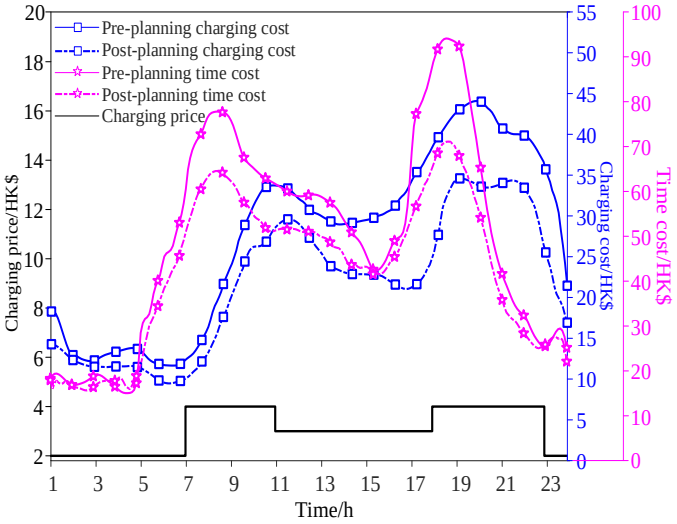

Figure 9. Average traveling and charging costs of users of pre-post-planning.

Table 2. Comparison of indicators of pre-post-planning.

Indicator	Pre-Planning	Post-Planning
Charging cost/HKD	27.43	25.79
Time cost/HKD	50.44	42.74
Charging waiting time/min	7.88	3.25
Charging traveling time/min	16.92	14.18
Utilization rate of charging pile/%	78.22	85.27

5.5. Comparison of Different Planning Methods

Finally, to comprehensively evaluate the effectiveness of the proposed hybrid planning, all charging piles at the 14 CSs are replaced with only fast and slow charging piles, establishing baseline methods, namely, fast and slow charging planning. Figures 10 and 11 illustrate the distribution network loads and voltage curves at 11:45 for different planning methods. The figures indicate that, for the slow-charging planning method, daytime loads are lower with charging loads concentrated in the evening and early morning hours. The evening peak of the distribution network occurs at 22:00, reaching 25.15 MW. In contrast, for the fast-charging planning method, loads are primarily concentrated between 10:00 and 17:00, with relatively low early morning loads. The peak-to-valley difference for the

entire day is as high as 15.19 MW. Conversely, the planning method proposed in this paper integrates various approaches based on different factors to create a comprehensive planning method. This method considers the charging characteristics and investment costs of different functional areas, reasonably distributing multiple types of charging piles to meet diverse charging demands while optimizing the load operation curve of the distribution network. The distribution network peaks at 11:45 a.m. with a load of 25.53 MW, dropping to a low of approximately 13.98 MW around 4:00 a.m. The peak-to-valley difference is reduced to 11.55 MW, representing a 23.96% decrease compared to the fast-charging planning method.

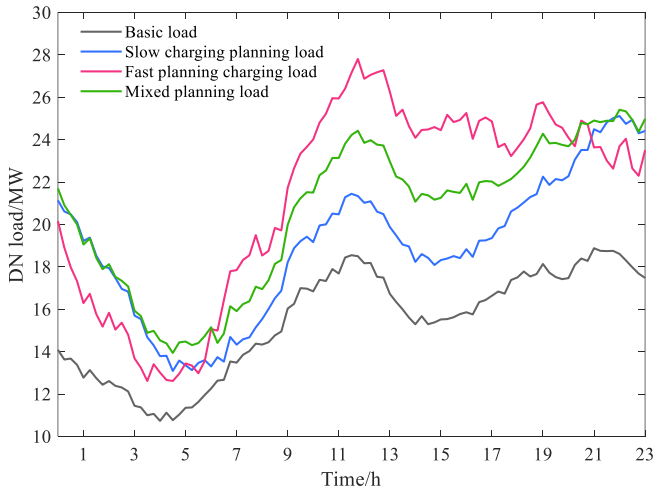

Figure 10. Comparison of distribution network loads for different planning methods.

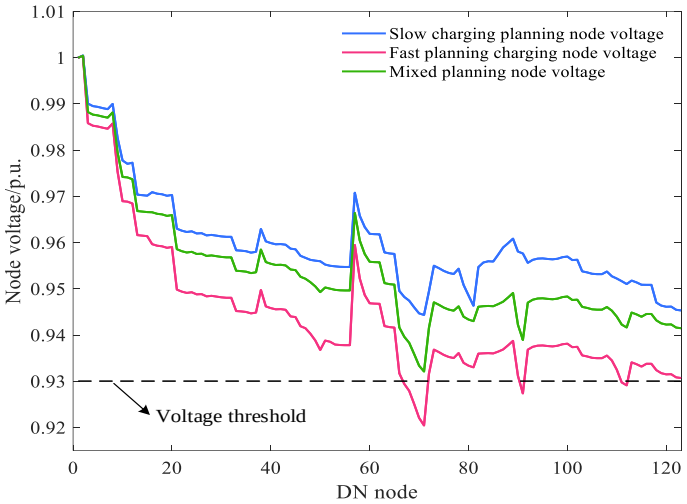

Figure 11. Comparison of node voltages for different planning methods.

Further, Table 3 shows the operational results under different planning methods. Combining Figure 11 and Table 3, the lowest point of the slow-charging method is 0.9444 p.u., with a voltage passing rate of 100% and an average user queuing time of 16.77 min. In contrast, the load of the fast-charging method peaks at 27.80 MW at 11:45, causing voltage overruns at some nodes. The minimum voltage drops to 0.9204 p.u., resulting in a voltage pass rate of only 99.81% for the entire day. The proposed method maintains a minimum voltage of 0.9321 p.u., ensuring a 100% voltage passing rate. The average user queuing time is reduced to 3.86 min, a 76.98% decrease compared to the slow-charging planning, significantly enhancing the charging experience for EV users.

Table 3. Comparison of indicators of different planning methods.

Method	Load Peak-Valley Difference/MW	Network Loss Rate/%	Minimum Voltage/p.u.	Voltage Pass Rate/%	Average Queuing Duration/min	Average Cost per User/HK$
Slow charging planning	12.03	4.15	0.9444	100	16.77	19.29
Fast charging planning	15.19	6.71	0.9204	99.81	7.21	33.54
Hybrid planning	11.55	4.49	0.9321	100	3.86	21.78

6. Conclusions

1. This study proposes a multi-stage hybrid planning method for CSs based on GAE. Firstly, the GAE-based deep learning method is used to identify the type of CSs for massive topological nodes, and then the planning decision-making model is built based on the traditional swarm intelligence optimization method, solving the problem of optimal location and capacity of CSs. Case studies in Kowloon City District of Hong Kong prove that the proposed method has the ability for accurate classification and efficient decision-making in complex network environments. Based on the proposed planning scheme, the average time cost of users is decreased by 15.27%, which not only significantly alleviated the charging congestion but also improved the utilization rate of urban charging piles. Compared with the peak charging demand before planning, the peak charging demand after planning is reduced by 37.51%, which effectively reduces the pressure of urban power grid operation. It provides support for the sustainable development of urban transportation-charging systems.
2. The research results will help the power and transportation departments to reasonably plan the layout of charging infrastructure, determine the number and location of different types of CSs, realize the optimal allocation of charging resources, and avoid the waste or shortage of resources. Also, the research results can effectively guide the EV users to charge orderly, reduce the charging cost of users, and reduce the operation pressure of the peak load of the urban power grid.
3. Although this study achieves certain results, there are still some limitations:
   Firstly, the scale of data used in the research needs to be expanded. More personalized behavioral data will help improve the scalability and adaptability of planning models, enhancing their ability to respond to complex decisions.
   Secondly, the deep learning method used in the research has the problem of time-consuming training. The computational complexity of the model is high in processing large-scale multidimensional variable feature data. More efficient processing algorithms will be developed to adapt to the rapid expansion of the EV market and the dynamic evolution of charging needs.
   Finally, the economic benefit analysis of CS planning in the research is relatively preliminary. In the future, we can further deepen the cost-benefit analysis and consider more economic and social factors, such as differentiated user behavior, fluctuations in land acquisition costs, and equipment maintenance and renewal costs, optimizing resource allocation and maximizing user satisfaction.

Author Contributions: Methodology, A.Y.W. and J.W.; Formal analysis, Y.-y.L. All authors have read and agreed to the published version of the manuscript.

Funding: This work described in this paper was supported by (1) a grant from the Research Grants Council of the Hong Kong Special Administrative Region, China (RGC Project Ref No. UGC/FDS24/E08/21), (2) the Chunhui Project Foundation of the Education Department of China.

Data Availability Statement: The original contributions presented in this study are included in the article. Further inquiries can be directed to the corresponding author.

Conflicts of Interest: Andrew Y. Wu and Yui-Yip Lau were employed by School of Professional Education and Executive Development, The Hong Kong Polytechnic University. Juai Wu was employed by College of Automation & College of Artificial Intelligence, Nanjing University of Posts and Telecommunications. The authors declare that the research was conducted in the absence of any commercial or financial relationships that could be construed as a potential conflict of interest.

Appendix A

Table A1. Main parameters of algorithmic model.

Parameter Configuration	Value
Charging infrastructure development costs	HKD 100 10,000/seat
Discount rate	0.08
Planning cycle	20 years
Unit price of fast charging piles	HKD 10 100,000/unit
Unit price of medium charging piles	HKD 6 100,000/unit
Unit price for slow charging piles	HKD 2 100,000/unit
Charging power of fast charging piles	120 kW
Charging power of medium charging piles	60 kW
Unit price for slow charging piles	20 kW
Unit time cost of urban travel	30 HKD/h
User queuing cost per hour	HKD 17
Conversion factor	0.1

References

1. Fescioglu-Unver, N.; Aktaş, M.Y. Electric vehicle charging service operations: A review of machine learning applications for infrastructure planning, control, pricing and routing. *Renew. Sustain. Energy Rev.* **2023**, *188*, 113873. [CrossRef]
2. Mo, T.; Lau, K.-T.; Li, Y.; Poon, C.-K.; Wu, Y.; Chu, P.K.; Luo, Y. Commercialization of Electric Vehicles in Hong Kong. *Energies* **2022**, *15*, 942. [CrossRef]
3. Woo, H.; Son, Y.; Cho, J.; Kim, S.Y.; Choi, S. Optimal expansion planning of electric vehicle fast charging stations. *Appl. Energy* **2023**, *342*, 121116. [CrossRef]
4. Tao, Y.; Qiu, J.; Lai, S.; Sun, X.; Zhao, J. Adaptive Integrated Planning of Electricity Networks and Fast Charging Stations Under Electric Vehicle Diffusion. *IEEE Trans. Power Syst.* **2023**, *38*, 499–513. [CrossRef]
5. Zhang, H.; Hu, Z.; Xu, Z.; Song, Y. Optimal Planning of PEV Charging Station with Single Output Multiple Cables Charging Spots. *IEEE Trans. Smart Grid* **2017**, *8*, 2119–2128. [CrossRef]
6. Yang, W.; Liu, W.; Chung, C.Y.; Wen, F. Joint Planning of EV Fast Charging Stations and Power Distribution Systems with Balanced Traffic Flow Assignment. *IEEE Trans. Ind. Inform.* **2021**, *17*, 1795–1809. [CrossRef]
7. Wang, W.; Liu, Y.; Wei, W.; Wu, L. A Bilevel EV Charging Station and DC Fast Charger Planning Model for Highway Network Considering Dynamic Traffic Demand and User Equilibrium. *IEEE Trans. Smart Grid* **2024**, *15*, 714–728. [CrossRef]
8. Wang, X.; Shahidehpour, M.; Jiang, C.; Li, Z. Coordinated Planning Strategy for Electric Vehicle Charging Stations and Coupled Traffic-Electric Networks. *IEEE Trans. Power Syst.* **2019**, *34*, 268–279. [CrossRef]
9. Xiao, S.; Lei, X.; Huang, T.; Wang, X. Coordinated Planning for Fast Charging Stations and Distribution Networks Based on an Improved Flow Capture Location Model. *CSEE J. Power Energy Syst.* **2023**, *9*, 1505–1516. [CrossRef]
10. Zhou, G.; Dong, Q.; Zhao, Y.; Wang, H.; Jian, L.; Jia, Y. Bilevel optimization approach to fast charging station planning in electrified transportation networks. *Appl. Energy* **2023**, *350*, 121718. [CrossRef]
11. Li, K.; Shao, C.; Hu, Z.; Shahidehpour, M. An MILP Method for Optimal Planning of Electric Vehicle Charging Stations in Coordinated Urban Power and Transportation Networks. *IEEE Trans. Power Syst.* **2023**, *38*, 5406–5419. [CrossRef]
12. Liu, S.; Wang, L.; Hu, J.; Zhou, Z. A Stochastic Charging Station Deployment Model for Electrified Taxi Fleets in Coupled Urban Transportation and Power Distribution Networks. *IEEE Trans. Sustain. Energy* **2024**, *15*, 1138–1150. [CrossRef]
13. Zhao, Z.; Xu, M.; Lee, C.K.M. Capacity Planning for an Electric Vehicle Charging Station Considering Fuzzy Quality of Service and Multiple Charging Options. *IEEE Trans. Veh. Technol.* **2021**, *70*, 12529–12541. [CrossRef]
14. Schoenberg, S.; Buse, D.S.; Dressler, F. Siting and Sizing Charging Infrastructure for Electric Vehicles With Coordinated Recharging. *IEEE Trans. Intell. Veh.* **2023**, *8*, 1425–1438. [CrossRef]
15. Ferro, G.; Minciardi, R.; Parodi, L.; Robba, M. Optimal Location and Line Assignment for Electric Bus Charging Stations. *IEEE Syst. J.* **2023**, *17*, 1950–1961. [CrossRef]

16. Li, C.; Dong, Z.; Chen, G.; Zhou, B.; Zhang, J.; Yu, X. Data-Driven Planning of Electric Vehicle Charging Infrastructure: A Case Study of Sydney, Australia. *IEEE Trans. Smart Grid* **2021**, *12*, 3289–3304. [CrossRef]
17. He, C.; Zhu, J.; Lan, J.; Li, S.; Wu, W.; Zhu, H. Optimal Planning of Electric Vehicle Battery Centralized Charging Station Based on EV Load Forecasting. *IEEE Trans. Ind. Appl.* **2022**, *58*, 6557–6575. [CrossRef]
18. Tao, Y.; Qiu, J.; Lai, S.; Sun, X.; Zhao, J. A Data-driven Agent-based Planning Strategy of Fast-Charging Stations for Electric Vehicles. *IEEE Trans. Sustain. Energy* **2023**, *14*, 1357–1369. [CrossRef]
19. Zhang, C.; Liu, Y.; Wu, F.; Tang, B.; Fan, W. Effective Charging Planning Based on Deep Reinforcement Learning for Electric Vehicles. *IEEE Trans. Intell. Transp. Syst.* **2021**, *22*, 542–554. [CrossRef]
20. Adil, M.; Mahmud, M.A.P.; Kouzani, A.Z.; Khoo, S.Y. Optimal Energy Trade in Retailer, Charging Station, and Electric Vehicles using a Stackelberg Game. In Proceedings of the 2023 IEEE IAS Global Conference on Renewable Energy and Hydrogen Technologies, GlobConHT 2023, Male, Maldives, 11–12 March 2023; Institute of Electrical and Electronics Engineers Inc.: Piscataway, NJ, USA, 2023. [CrossRef]
21. Heo, J.; Chang, S. Optimal Planning for Electric Vehicle Fast Charging Stations Placements in a City Scale Using an Advantage Actor-Critic Deep Reinforcement Learning and Geospatial Analysis. *Sustain. Cities Soc.* **2024**, *113*, 105567. [CrossRef]
22. Huang, Q.; Zhou, G.; Wang, H.; Dong, Q.; Jia, Y. A Progressive Planning Scheme for Dynamic Expansion of Electric Vehicle Charging Resources. *IEEE Trans. Smart Grid* **2024**, *15*, 4946–4960. [CrossRef]
23. Wen, Y.; Cai, B.; Yang, X.X.; Xue, Y.S. Quantitative analysis of China's Low-Carbon energy transition. *Int. J. Electr. Power Energy Syst.* **2020**, *119*, 1–9. [CrossRef]
24. Xing, Q.; Xu, Y.; Chen, Z. A Bilevel Graph Reinforcement Learning Method for Electric Vehicle Fleet Charging Guidance. *IEEE Trans. Smart Grid* **2023**, *14*, 3309–3312. [CrossRef]
25. Han, T.; Tang, Y.; Chen, Y.; Yang, X.; Guo, Y.; Jiang, S. SDC-GAE: Structural Difference Compensation Graph Autoencoder for Unsupervised Multimodal Change Detection. *IEEE Trans. Geosci. Remote Sens.* **2024**, *62*, 1–16. [CrossRef]
26. Wen, Y.; Cai, B.; Xue, Y.S.; Wang, S.M.; Chen, Z.L.; Zhu, J.M.; Jiang, D.L.; Yue, Z.Y. Assessment of Power System Low-carbon Transition Pathways Based on China's Energy Revolution Strategy. *Energy Procedia* **2018**, *152*, 1039–1044. [CrossRef]